

## Surface magnetic phase diagram for a semi-infinite ferromagnet

A. P. Popov

*Department of Molecular Physics, Moscow State Engineering Physics Institute, Kashirskoe shosse, 31, 115407 Moscow, Russia*

D. P. Pappas

*National Institute of Standards and Technology, Boulder, Colorado 80305*

(Received 4 May 2001; published 12 October 2001)

The phase diagram for the orientation of the surface region is calculated in the parameter space defined by the surface and bulk anisotropy in semi-infinite ferromagnetic systems and in thin ferromagnet films. Surface magnetic canting always occurs when the magnitude of the surface anisotropy is comparable with the interlayer exchange interaction. Increasing the thickness of a thin film supported on a hard magnetic substrate induces a spin reorientation transition from the uniform, in-plane magnetic structure to a canted state. The inverse spin reorientation transition from the canted state to the uniform, in-plane magnetic structure with thickness is demonstrated for a thin film supported on a nonmagnetic substrate. A discrete layer-by-layer approach is developed and compared to the continuum approach. We consider the 1.5 atomic-layer system of Fe on Gd and find that it is a good physical realization of the model.

DOI: 10.1103/PhysRevB.64.184401

PACS number(s): 75.70.-i, 75.70.Rf

### INTRODUCTION

Determining the equilibrium state of magnetic moments at surfaces and interfaces is key to understanding the magnetic behavior of semi-infinite systems. In particular, surfaces and interfaces can exhibit strong anisotropy,  $K_S$ , due to the reduced symmetry. It has been shown that  $K_S$  can favor either perpendicular or in-plane magnetization alignment.<sup>1</sup> This term competes with magnetocrystalline and dipole energy of the bulk system,  $K_B$ , which combined, can again favor either direction of bulk magnetization alignment. Consideration of these effects leads to the possibility that a domain-wall-like structure can exist in the surface region.<sup>2</sup> This would be manifested in a surface magnetic canting (SMC) with a gradual transition to the equilibrium magnetization in the bulk.

At present, it is generally believed that SMC takes place due to the difference between the surface and bulk anisotropy, characterized by the anisotropy constants  $K_S$  and  $K_B$ , respectively.<sup>2,3</sup> Leaving aside the problem of the origin of surface and bulk anisotropy, we find that the region in the phase diagram in coordinates  $(K_S, K_B)$  that encompasses SMC has, to date, not been determined.<sup>4-6</sup> The main goal of this article is to fill this gap in magnetic surface science.

We consider this problem in the framework of the simplest approach: a Heisenberg model with quasiclassical vector moments and an isotropic exchange interaction. In this model, the layer index  $n=1$  corresponds to the top surface atomic layer, where a second-order anisotropy is assigned with anisotropy constant  $K_S$ . All of the inner layers ( $n=2, 3, \dots, N$ ) are considered to be bulklike, with second-order anisotropy characterized by constant  $K_B$ , which is independent of the layer index  $n$ . In addition we include an interlayer ferromagnetic exchange  $J_{n,n+1} \equiv J > 0$ . Within this approach, the problem is reduced to the consideration of a one-dimensional chain, and thus the energy  $E$  may be written as

$$E = -J \sum_{n=1}^N \cos(\theta_n - \theta_{n+1}) + K_S \sin^2 \theta_1 + K_B \sum_{n=2}^N \sin^2 \theta_n, \quad (1)$$

where  $\theta_n$  is the angle between the  $n$ th layer vector moment and the surface plane as shown in Fig. 1. Below we consider the case of a semi-infinite crystal ( $N \rightarrow \infty$ ) in Secs. I–III, V, and VI and also thin films with a finite number of layers,  $N$ , in Sec. IV.

We demonstrate that the onset of SMC follows the criterion for instability of a uniform magnetic structure. This is similar to the approach used in Ref. 7. Within this model we express this criterion in terms of the model parameters in closed form. Basing on this result we build a phase diagram in coordinates of reduced-anisotropy constants

$$k_S \equiv \frac{2K_S}{J}, \quad k_B \equiv \frac{2K_B}{J},$$

which show the regions corresponding to SMC. We propose its physical treatment for the cases where  $k_S < 0$ ,  $k_B > 0$  and  $k_S > 0$ ,  $k_B < 0$  in Sec. I and Sec. II, respectively. Of particular interest is the region where the surface is always canted, i.e.,

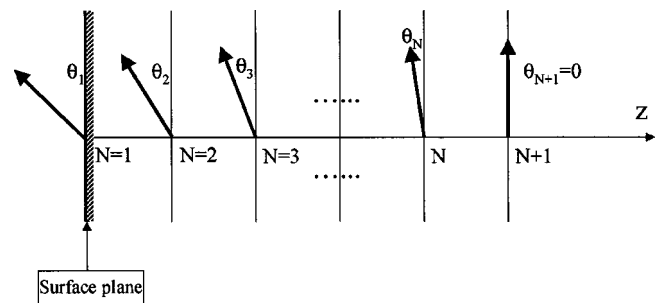


FIG. 1. Discrete layer model used for the semi-infinite ferromagnet exhibiting a bulk in-plane anisotropy and a surface perpendicular anisotropy. Surface magnetic canting is shown.

where SMC takes place regardless of how large the magnitude of reduced-bulk-anisotropy constant  $k_B$  is. This case is discussed in Sec. II.

In Sec. III we derive the evolution of the borders in the  $(k_S, k_B)$  phase diagram with an external magnetic field  $h$ . We show that in the case  $k_S < 0, k_B > 0$  accounting for an in-plane magnetic field leads to a finite interval in  $k_S$  where the appearance of SMC is suppressed. Thus, in this case there is some threshold magnitude of  $k_S$  for the appearance of SMC. Similar results are obtained for the case  $k_S > 0, k_B < 0$ .

In Sec. IV this method is then applied to thin magnetic films, and it is shown that the finite thickness of a film supported on a hard magnetic substrate gives rise to a decrease in the SMC region in the  $(k_S, k_B)$  phase diagram. In this case, for a suitable set of magnitudes of model parameters, the spin reorientation transition (SRT) from an in-plane uniform magnetic structure to the SMC structure takes place. In contrast, the finite thickness of a film supported on a non-magnetic substrate gives rise to a decrease in the SMC region in the  $(k_S, k_B)$  phase diagram. In this case, for a suitable set of magnitudes of model parameters, the SRT from a SMC structure to the in-plane uniform magnetic structure takes place.

In Sec. V we compare our results with the description of SMC obtained within the continuum approach.<sup>2,3</sup> We show that, from the viewpoint of the  $(k_S, k_B)$  phase diagram, results obtained within the continuum approach correspond to ours in only a narrow range of model-parameter magnitudes. A method for improvement on the continuum approach model is proposed.

We discuss the relevance of this model to real physical systems. In particular, in Sec. VI we treat the case of 1.5 atomic-layer films of Fe on Gd that have been shown to demonstrate the SRT from the in-plane to SMC structure.

### I. PHASE DIAGRAM FOR SURFACE MAGNETIC CANTING IN SEMI-INFINITE FERROMAGNET: PERPENDICULAR SURFACE ANISOTROPY AND IN-PLANE BULK ANISOTROPY

For a semi-infinite ferromagnet exhibiting a bulk in-plane anisotropy, the appearance of SMC is marked by a small deviation of the first few layer vector moments from the

in-plane orientation. SMC takes place only when it becomes energetically favorable compared to the uniform in-plane structure. Therefore, the evaluation for the criterion of SMC implies that each angle  $\theta_n$  in Eq. (1) has to be varied away from zero, and the resulting perturbation on the energy evaluated. For the case of small deviations of  $\theta_n$ , the expression for energy in Eq. (1) may be expanded to second order for each  $\theta_n$ ,

$$E \approx E_0 + \boldsymbol{\theta}^T A \boldsymbol{\theta}, \quad \boldsymbol{\theta} = (\theta_1, \theta_2, \dots, \theta_N). \quad (2)$$

Here  $E_0$  is a part of the energy-independent  $\theta_n$  and  $A$  is a square  $(N \times N)$  three-diagonal symmetric matrix with real elements. The set of  $N$  eigenvectors,  $\mathbf{a}_n$ , of this matrix represents a full set of orthogonal vectors, i.e., they form a basis in  $N$ -dimensional space. Therefore, it is possible to expand the vector  $\boldsymbol{\theta}$  in eigenvectors  $\mathbf{a}_n$ ,

$$\boldsymbol{\theta} = c_1 \mathbf{a}_1 + c_2 \mathbf{a}_2 + \dots + c_N \mathbf{a}_N. \quad (3)$$

Equation (2) may then be rewritten as

$$E = E_0 + \sum_n^N \Lambda_n |c_n|^2. \quad (4)$$

Here  $\Lambda_n$  is the  $n$ th eigenvalue of matrix  $A$ . In order to minimize the energy defined by Eq. (4) one must vary the coefficients  $c_n$  that determine the canting profile in accordance with Eq. (3). Therefore, for a given set of magnitudes of model parameters,  $K_S$ ,  $K_B$ ,  $J$ , and  $N$ , the minimal energy  $E$  corresponds to a certain magnetic structure in the surface region. From Eq. (4) we find that for only positive signs of each eigenvalue  $\Lambda_n$  the energy is minimized when every  $|c_n|^2 = 0$ . This corresponds to  $\boldsymbol{\theta} = 0$ , i.e., a uniform magnetic structure with an in-plane orientation of each layer's vector moment. However, if even one  $\Lambda_n$  becomes negative, then the condition  $\boldsymbol{\theta} = 0$  does not correspond to an energy minimum. In this case, a uniform magnetic structure with an in-plane orientation of each layer vector moment is not the stable configuration. Hence, the criterion for SMC is that the minimal eigenvalue of the matrix  $A$  should be less than zero.

In order to express this criterion, first one needs to find this minimal eigenvalue  $\Lambda_{\min}$ , express it in terms of model parameters, and then solve the inequality  $\Lambda_{\min} < 0$ . The equation for eigenvalues of the matrix  $A$  is expressed as

$$\det |A - \Lambda I| = J^N \det \begin{vmatrix} \varepsilon_\lambda + \kappa/2 & -\frac{1}{2} & 0 & 0 & 0 & 0 \\ -\frac{1}{2} & \varepsilon_\lambda & -\frac{1}{2} & 0 & 0 & 0 \\ 0 & -\frac{1}{2} & \varepsilon_\lambda & -\frac{1}{2} & 0 & 0 \\ 0 & 0 & -\frac{1}{2} & \varepsilon_\lambda & -\frac{1}{2} & 0 \\ 0 & 0 & 0 & -\frac{1}{2} & \varepsilon_\lambda & -\frac{1}{2} \\ 0 & 0 & 0 & 0 & -\frac{1}{2} & \varepsilon_\lambda \end{vmatrix} = 0. \quad (5)$$

Here,  $\varepsilon_\lambda = 1 + (K_B/J) - \lambda = \varepsilon - \lambda$ ,  $\lambda = \Lambda/J$ ,  $\kappa = -1 + 2(K_S - K_B)/J$ . The parameter  $\kappa$  characterizes the surface perturbation that originates from both the absence of the outer layer above the surface and the difference between the surface,  $K_S$ , and bulk,  $K_B$ , anisotropy constants. Because we consider the case of a semi-infinite crystal ( $N \rightarrow \infty$ ) in this section, we neglect the surface perturbation at the other surface of a film, i.e., in the bottom right corner of the matrix the parameter  $\kappa$  is set to zero. Equation (5) can then be written in the form

$$d_N + \frac{k}{2} d_{N-1} = 0. \quad (6)$$

Here,  $d_N$  is the determinant of an ( $N \times N$ ) matrix similar to Eq. (5) but with all diagonal elements equal to  $\varepsilon_\lambda$ , i.e.,  $\kappa = 0$ . For various values of  $\varepsilon_\lambda$ , the determinant  $d_N$  can have various forms.<sup>7</sup> Because the expression for  $\varepsilon_\lambda$  contains the reduced eigenvalue  $\lambda = \Lambda/J$ , the form of Eq. (6) depends on the interval over which the eigenvalue is searched for. This means that while searching for eigenvalues we must consider all possible cases.

Case (i)  $|\varepsilon_\lambda| \leq 1$ . In this case the reduced eigenvalues belong to a “band,” i.e.,

$$-1 \leq \varepsilon - \lambda \leq +1,$$

or equivalently,

$$\frac{K_B}{J} \equiv \varepsilon - 1 \leq \lambda \leq \varepsilon + 1 \equiv \frac{K_B}{J} + 2. \quad (7a)$$

Since we consider the case where the bulk-anisotropy constant  $K_B$  favors in-plane magnetization,  $K_B$  is positive. Therefore, none of the eigenvalues from the “band” cross zero and this case can be ignored.

Case (ii)  $\varepsilon_\lambda < -1$ . This inequality may be rewritten as

$$2 < \frac{K_B}{J} + 2 \equiv \varepsilon + 1 < \lambda. \quad (7b)$$

Thus, similar to case (i), the eigenvalue will not cross zero and this case also can be discarded.

Case (iii)  $\varepsilon_\lambda > +1$ . This inequality may be rewritten as

$$\lambda < \varepsilon - 1 \equiv \frac{K_B}{J}. \quad (7c)$$

Therefore, case (iii) is the only one that gives a negative eigenvalue  $\lambda$ . In this case the determinant  $d_N$  has the following form:<sup>7</sup>

$$d_N = \frac{\sinh \varphi(N+1)}{2^N \sinh \varphi}, \quad \cosh \varphi = \varepsilon_\lambda, \quad 0 < \varphi. \quad (8)$$

Substitution of Eq. (8) into Eq. (6) gives rise to the following equation for the minimal eigenvalue:

$$-\kappa = \frac{\sinh \varphi(N+1)}{\sinh \varphi N}. \quad (9)$$

Because we consider here the semi-infinite crystal, Eq. (9) is simplified as

$$\lim_{N \rightarrow \infty} \frac{\sinh \varphi(N+1)}{\sinh \varphi N} = \exp(\varphi) = -\kappa. \quad (10)$$

Since  $\varphi > 0$ , Eq. (10) has a solution only for  $\kappa < -1$ . In terms of the model parameters, this inequality means that  $K_S < K_B$ . This requirement is satisfied because  $K_S < 0$  and  $K_B > 0$ . Equation (10) allows one to obtain the expression for the eigenvalue  $\lambda$  in a closed form

$$\lambda = \varepsilon + \frac{1}{2} \left( \kappa + \frac{1}{\kappa} \right). \quad (11)$$

Finally, the inequality  $\lambda < 0$  may be written in terms of the model parameters. We find that the most convenient way to do this is to use the reduced-anisotropy constants  $k_S \equiv 2K_S/J$  and  $k_B \equiv 2K_B/J$ . In terms of  $k_S$  and  $k_B$ , the criterion for SMC can be written exactly in closed form as

$$k_S + 1 < \frac{1}{k_B - (k_S - 1)}. \quad (12)$$

For  $-1 < k_S < 0$ , the inequality of Eq. (12) is satisfied for  $k_B$  smaller than some threshold magnitude determined by the formula

$$k_B < k_S - 1 + \frac{1}{k_S + 1}. \quad (13)$$

For  $k_S < -1$  the inequality of Eq. (12) is satisfied for any positive magnitude of  $k_B$ . This shows that the surface is always canted when  $k_S < -1$ , independent of the bulk-anisotropy constant. This reflects the fact that SMC is driven by the relative strength of  $K_S$  and the interlayer exchange,  $J$ . The region corresponding to SMC in a semi-infinite ferromagnet exhibiting in-plane bulk anisotropy and perpendicular surface anisotropy is shown in the left upper corner of the ( $k_S, k_B$ ) phase diagram presented in Fig. 2.

## II. PHASE DIAGRAM FOR SURFACE MAGNETIC CANTING IN A SEMI-INFINITE FERROMAGNET: IN-PLANE SURFACE ANISOTROPY AND PERPENDICULAR BULK ANISOTROPY

The generalization of this result for the case of surface anisotropy favoring in-plane magnetization and bulk anisotropy  $K_B$  that favors magnetization perpendicular to the surface ( $k_S < 0, k_B < 0$ ) is straightforward. In this case one must revise the definition of SMC slightly because it corresponds to a magnetic structure with the layer vector moments deviated from the normal to the surface rather than from the in-plane direction. In accordance with this new definition of SMC it is more convenient to measure angles from the normal vector perpendicular to the surface. Thus we introduce angles  $\alpha_n = \pi/2 - \theta_n$  and expand the energy in Eq. (1) to second order of every  $\alpha_n$ . Then the expression for the reduced eigenvalue  $\lambda$  in Eq. (11) is valid. The difference is that now the reduced surface perturbation  $\kappa$  is determined by

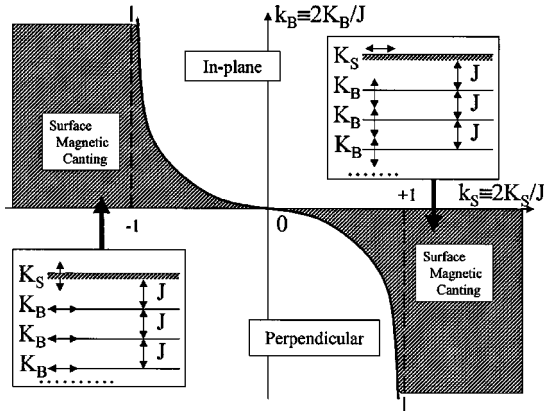


FIG. 2. Phase diagram for surface magnetic canting in the semi-infinite ferromagnet in coordinates of reduced-anisotropy constants ( $k_S, k_B$ ). The schematic representation of the model used for the description of SMC/in-plane border and SMC/perpendicular border is presented in two insets. The region corresponding to SMC in a semi-infinite ferromagnet exhibiting in-plane, bulk anisotropy, and perpendicular surface anisotropy is shown in the left upper corner of the phase diagram. The SMC/in-plane border is described by the Eq. (13). The region corresponding to SMC in a semi-infinite ferromagnet with perpendicular bulk anisotropy and in-plane surface anisotropy is shown in the bottom right corner of the ( $k_S, k_B$ ) phase diagram. The SMC/perpendicular border is described by Eq. (15).

$$\kappa = -1 + \frac{2(K_S - K_B)}{J}.$$

As a consequence, in terms of  $k_S$  and  $k_B$  the criterion for the appearance of SMC in the surface region of the bulk ferromagnetic has the form

$$\frac{1}{k_B - (k_S + 1)} < k_S - 1. \quad (14)$$

The analysis of this inequality for  $k_B < 0$  and  $k_S > 0$  shows the following. For  $0 < k_S < 1$ , the inequality of Eq. (14) is satisfied when  $k_B$  is negative and larger than some threshold magnitude determined by formula

$$k_S + 1 + \frac{1}{k_S - 1} < k_B. \quad (15)$$

For  $k_S > 1$ , the inequality of Eq. (13) is satisfied for arbitrarily large negative  $k_B$ . The region corresponding to SMC in a semi-infinite ferromagnet with perpendicular bulk anisotropy and in-plane surface anisotropy is shown in the bottom right corner of the ( $k_S, k_B$ ) phase diagram presented in Fig. 2. The cases  $k_S, k_B > 0$  and  $k_S, k_B < 0$  do not give rise to any kind of SMC.

Below we present the physical treatment of the phase diagram obtained. An important common feature of the two parts of the phase diagram that exhibit SMC is the existence of regions that always have SMC independent of the bulk anisotropy determined by the inequality  $|k_S| > 1$ . The existence of this region bordered in the left upper part of the phase diagram by the asymptote  $k_S = -1$  may be best understood within the limiting case of  $k_B \rightarrow \infty$ . In this case, each

bulk vector moment ( $n=2,3,\dots$ ) is oriented in-plane. Therefore, the problem is reduced to a one-layer approach and may be easily investigated analytically. Equation (1) then has the form

$$E_1 = -J \cos \theta_1 + K_S \sin^2 \theta_1.$$

Minimization of  $E_1$  with respect to angle  $\theta_1$  gives the solutions

$$\sin \theta_1 = 0 \Rightarrow \theta_1 = 0$$

and

$$\cos \theta_{1C} = -\frac{J}{2K_S} \Rightarrow \theta_{1C} = \arccos\left(-\frac{J}{2K_S}\right)$$

The difference between the energies corresponding to these solutions is determined by the formula

$$\Delta E_1 = E_1(\theta_1 = \theta_{1C}) - E_1(\theta_1 = 0) = \frac{(J + 2K_S)^2}{4K_S}.$$

Since we present here the physical treatment of the case of perpendicular surface anisotropy considered in Sec. I, the anisotropy constant  $K_S$  is negative. Therefore, the energy difference  $\Delta E_1$  is also negative and the state with SMC is always favorable. However, the deviation of the surface moment is determined by the formula  $\cos \theta_1 = -J/2K_S \equiv -1/k_S$ . Therefore, SMC may be realized only for those magnitudes of  $k_S$  that correspond to  $\cos \theta_1 < 1$ , i.e.,  $k_S < -1$ . Also, in this particular case, the susceptibility  $\chi_\perp$  with respect to perpendicular magnetic field may be calculated, and is given by

$$\chi_\perp(k_S > -1) = \frac{1}{2(k_S + 1)},$$

$$\chi_\perp(k_S < -1) = \frac{1}{2(k_S + 1)k_S(1 - k_S)}. \quad (16)$$

It follows from these two formulas that in the vicinity of the border between the canted and in-plane states of the surface, both  $\chi_\perp(k_S < -1)$  and  $\chi_\perp(k_S > -1)$  diverge. In addition  $\chi_\perp(k_S > -1) = 2\chi_\perp(k_S < -1)$ , demonstrating that the transition from in-plane surface magnetization to canted is of second order. This applies to all of the borders in the phase diagram in Fig. 2. These results and the existence of regions where the surface is always canted might be best understood in this limiting case because, for  $k_B \rightarrow \infty$ , the orientation of the surface vector moment is affected only by the exchange interaction between the first and second layers and the surface anisotropy  $K_S$ . The rotation of the surface vector moment to  $90^\circ$  from an in-plane to out-of-plane orientation gives rise to an increase in the energy of exchange interaction of the surface moment with the subsurface one. On the other hand, this rotation will give rise to an increase in the surface-anisotropy energy. If the latter is larger than the exchange-interaction energy then the surface-vector moment will deviate from an in-plane orientation. The physical treat-

ment of the region in the right bottom corner of the phase diagram where the surface is always canted is similar.

### III. EFFECT OF EXTERNAL MAGNETIC FIELD ON THE PHASE DIAGRAM

After establishing that equations of all lines in the magnetic surface diagram can be obtained in closed form, Eqs. (12)–(15), we now turn to the case with nonzero applied magnetic field,  $h \neq 0$ . In the case where  $k_S < 0, k_B > 0$ , accounting for an in-plane external magnetic field  $h_{\parallel}$  gives rise to an additional term in the energy  $E$ ,

$$E = -J \sum_{n=1}^N \cos(\theta_n - \theta_{n+1}) + K_S \sin^2 \theta_1 + K_B \sum_{n=2}^N \sin^2 \theta_n - \sum_{n=1}^N h_{\parallel} \cos \theta_n. \quad (17)$$

In this case, the procedure for finding the minimal eigenvalue is the same. This is due to the fact that matrix  $A$  has the same form because the surface perturbation  $\kappa$  is the same. Similarly, Eq. (11) for  $\lambda$  is also valid. However, the parameter  $\varepsilon$  changes to  $\varepsilon = 1 + k_S/2 + h_{\parallel}/2$ . As a consequence, the criterion for uniform magnetic structure to be unstable has a different form,

$$k_S + 1 + h_{\parallel} < \frac{1}{k_B - (k_S - 1)}. \quad (18)$$

Analysis of this formula shows that including  $h_{\parallel}$  leads to an increase of the in-plane region in the  $(k_S, k_B)$  phase diagram. The details of the movement of the SMC-in-plane border are as follows. First, the asymptote at  $k_S = -1$  moves to the left because it is determined by the formula  $k_S = -1 - h_{\parallel}$ . Second, accounting for an in-plane magnetic field leads to the existence of a finite interval in  $k_S$  where SMC is forbidden for  $k_B = 0$ . Therefore, in this case, the SMC is suppressed and appears only if  $k_S$  exceeds some critical magnitude determined by the formula

$$k_S < k_{SC\parallel} = -\frac{h_{\parallel} + \sqrt{h_{\parallel}^2 + 4h_{\parallel}}}{2}. \quad (19a)$$

The border between SMC and in-plane regions for  $h \neq 0$  is shown in the phase diagram of Fig. 3. Accounting for an external magnetic field  $h_{\perp}$  perpendicular to the surface plane for  $k_S > 0, k_B < 0$  leads to similar consequences in the bottom right part of the phase diagram, as shown. The expression for  $k_{SC\perp}$  is determined by the formula

$$k_S > k_{SC\perp} = +\frac{h_{\perp} + \sqrt{h_{\perp}^2 + 4h_{\perp}}}{2}. \quad (19b)$$

### IV. THIN-FILM MAGNETISM

In the case of a finite number of layers,  $N$ , in a thin film one first must take into account the surface perturbation at the other surface of a film in Eq. (5) and, second, solve the resulting equation without the assumption  $N \rightarrow \infty$ . The solu-

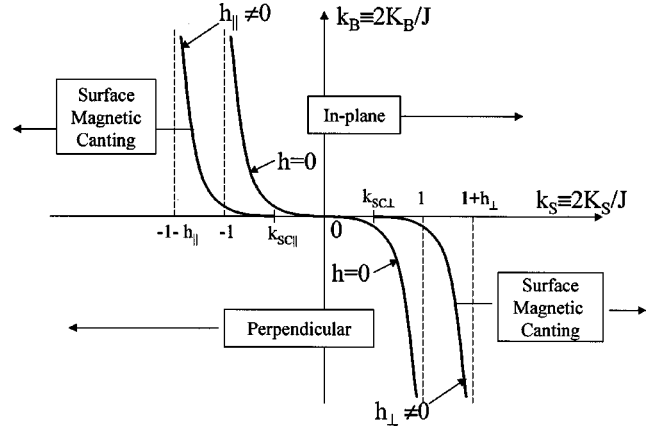


FIG. 3. The evolution of SMC/in-plane border, Eq. (19a), in the  $(k_S, k_B)$  phase diagram with an in-plane magnetic field  $h_{\parallel}$  is shown in the left upper corner of the phase diagram. The evolution of SMC/perpendicular border, Eq. (19b), with perpendicular magnetic field  $h_{\perp}$  is shown in the bottom right corner of the phase diagram. The parameters  $k_{SC\parallel}$  and  $k_{SC\perp}$  confine the intervals in  $k_S$  where SMC is forbidden for  $k_B = 0$ .

tion of Eq. (5) for a finite number of atomic layers is of special interest in thin-film magnetism. However, the necessity to account for a surface perturbation on each side of the film brings additional complications. For the sake of simplicity, we consider two extreme cases: (A) a thin film supported on a magnetic substrate that has an extremely small depth of SMC and (B) a thin film supported on nonmagnetic substrate.

Case (A). In this limiting case, Eq. (9) is valid because the surface perturbation on the other plane of the film is already taken into account, i.e.,  $\theta_n = 0$  for  $n > N$  (see Fig. 1). Then, the right side of Eq. (9) may be written as

$$\begin{aligned} -\kappa &= \frac{\sinh \varphi(N+1)}{\sinh \varphi N} \\ &= \exp(\varphi) + [\exp(\varphi) - \exp(-\varphi)] \frac{\exp(-2\varphi N)}{1 - \exp(-2\varphi N)} \\ &\approx \exp(\varphi) + [\exp(\varphi) - \exp(-\varphi)] \exp(-2\varphi N). \end{aligned} \quad (20)$$

One can see from this formula that the correction to our previous result, Eq. (10), obtained for a semi-infinite crystal in the limit  $N \rightarrow \infty$  decreases exponentially with the thickness of the film. What is more important is that this correction is positive in the interval  $0 < \varphi < +\infty$ . The latter gives rise to the following consequence: Eq. (19) is satisfied with a smaller magnitude of  $\varphi$  for any given value of the parameter  $-\kappa$ . Bearing in mind the relation  $\lambda = \varepsilon - \cosh(\varphi)$  [see definitions of parameters  $\varepsilon$ ,  $\varepsilon_{\lambda}$ , and  $\varphi$  in Eqs. (5) and (8)], one may conclude that accounting for a finite number of layers gives rise to a decrease in the parameter  $\varphi$ , and this, in turn, leads to an increase in the minimal eigenvalue  $\lambda$ . As a consequence,  $\lambda$  crosses zero later because in order to satisfy the requirement  $\lambda = 0$ , one needs a larger surface anisotropy compared to that of a semi-infinite crystal. Therefore, the

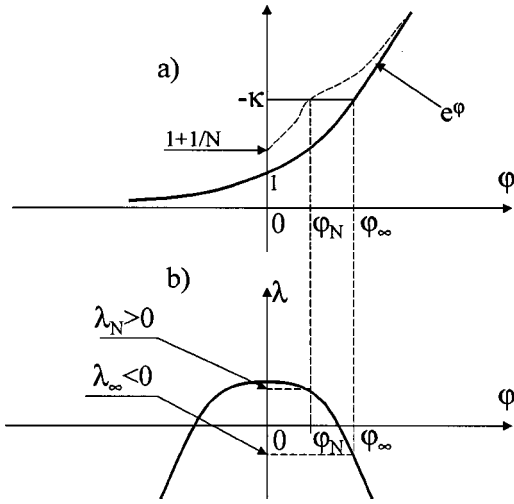


FIG. 4. (a) Graphical solution of Eq. (10) for the parameter  $\varphi$  corresponding to minimal eigenvalue of the matrix  $A$  in Eq. (5) for semi-infinite ferromagnet (solid line) and Eq. (20) for  $N$ -layer film supported on a hard magnetic substrate (dashed line). (b) Graphical illustration of the case when the criterion for SMC in a semi-infinite ferromagnet is fulfilled ( $\lambda_\infty < 0$ ), but in  $N$ -layer film with the same magnitudes of model parameter  $k_S, k_B$  not fulfilled ( $0 < \lambda_N$ ). The suppression of SMC in thin magnetic films is essentially a thin-film effect because the additional effective in-plane anisotropy in an  $N$ -layer film exists exclusively due to the finite thickness of this film only. This effect cannot be assigned to either the surface-anisotropy constant or the bulk one and thus needs to be accounted for directly in the treatment of SRT in thin films supported on a hard magnetic substrate.

appearance of SMC in a thin film supported on the hard magnetic substrate is suppressed. This situation is illustrated in Fig. 4.

Below we evaluate this solution for a few different film thicknesses  $N$ .

$N=1$ . In this case, the problem is restricted to the one-layer approach that was considered in Sec II. Now, SMC must be treated as a deviation of the monolayer vector moment from the in-plane orientation. SMC takes place for  $k_S < -1$  and thus the region of SMC coincides with the region where the surface is always canted in the phase diagram of Fig. 2. For  $-1 < k_S < 0$ , the monolayer vector moment is always parallel to the surface.

$N=2$ . In this case, the region of SMC is larger than that of  $N=1$ . If  $k_S < -1$ , then, similarly to  $N=1$ , SMC takes place whenever  $k_B > 0$ , while for  $k_S > -1$  SMC occurs only when  $k_B$  satisfies the inequality

$$k_B < \frac{-2k_S - 1}{k_S + 1}. \quad (21)$$

The right side of Eq. (21) is negative for  $-\frac{1}{2} < k_S < 0$ , and thus we may conclude that the range of  $k_S$  where SMC is suppressed becomes half as large as in the  $N=1$  case.

$N=3$ . Similar to the cases  $N=1$  and  $N=2$ , for  $k_S < -1$  the SMC occurs whenever  $k_B > 0$ . For  $k_S > -1$  the SMC occurs only when  $k_B$  satisfies the inequality

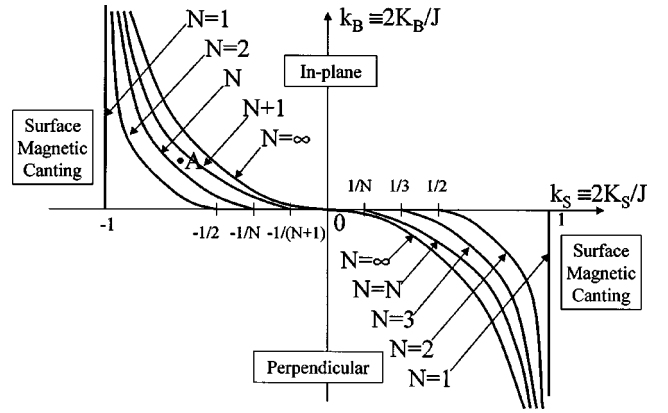


FIG. 5. Evolution of SMC/in-plane and SMC/perpendicular borders in the  $(k_S, k_B)$  phase diagram with the increase in thickness of a thin film supported on a hard magnetic substrate. Point  $A$  in the left upper corner of the phase diagram is located in an in-plane region for an  $N$ -layer film. However the point  $A$  with the same coordinates  $(k_S, k_B)$  is located in the SMC region for an  $(N+1)$ -layer film. This illustrates the SRT from an in-plane uniform magnetic structure of the  $N$ -layer film to SMC in the  $(N+1)$ -layer film with the increase in thickness.

$$k_B > \frac{-4k_S - 3 + \sqrt{4k_S^2 + 8k_S + 5}}{2(k_S + 1)}. \quad (22)$$

It follows from Eq. (22) that the evolution of the border is the same, i.e., the SMC region continues its extension and now the SMC/in-plane border crosses the  $k_B=0$  axis at  $k_S = -\frac{1}{3}$ .

A common feature of all the lines that determine the SMC/in-plane border in the phase diagram for thin films with  $N=1, 2, 3, \dots$  supported on a hard magnetic substrate is that each of these lines has an asymptote at  $k_S = -1$ . This line moves to the right side of the diagram as  $N$  increases and crosses the axis  $k_B=0$  at  $k_S = -1/N$  (Fig. 5). In the limiting case  $N \gg 1$ , the SMC/in-plane border coincides with that obtained within the assumption  $N \rightarrow \infty$  [Eq. (13)]. This result may be treated as a qualitative description of a SRT in a thin film as the thickness increases. Indeed, while an  $N$ -layer film, with surface-anisotropy constant  $k_S$  satisfying the inequality  $1/N < k_S < 1/(N+1)$  and small  $k_B$ , exhibits an in-plane orientation, the  $(N+1)$  layer film with the same  $k_S$  and  $k_B$  exhibits SMC. Therefore, we find a SRT from an in-plane to SMC with increasing thickness of the film deposited on a magnetic substrate with an extremely small depth of SMC.

These trends may be understood in the following way. The existence of an asymptote at  $k_S = -1$  in each curve for  $N=1, 2, 3, \dots$  shows that the surface vector moment is always canted when the surface anisotropy exceeds the exchange interaction with the subsurface layer. In this case, the canted state always exists. The increase in the range of  $k_S$  where canting is suppressed for ultrathin films is a consequence of reduced thickness of a film, which is insufficient to support a SMC state that is suppressed in the hard magnetic substrate, i.e., in the layers with layer index  $n=N+1, N+2, \dots$ .

Case (B). To consider the case corresponding to a thin magnetic film supported on a nonmagnetic substrate, one must take into account the surface perturbation  $\kappa$  at the other surface of a film, i.e., one must substitute  $\varepsilon_\lambda + \kappa$  instead of  $\varepsilon_\lambda$  in the bottom right corner of matrix  $A$  in Eq. (5). The equation for the eigenvalues can then be written in the form

$$d_N + \kappa d_{N-1} + \frac{\kappa^2}{4} d_{N-2} = 0. \quad (23)$$

The substitution of the expression for  $d_N$  determined by the Eq. (8), into Eq. (23) gives rise to the equation

$$1 + 2\kappa \frac{\sinh \varphi N}{\sinh \varphi(N+1)} + \kappa^2 \frac{\sinh \varphi(N-1)}{\sinh \varphi(N+1)} = 0. \quad (24)$$

First, it follows from Eq. (24) that in the limiting case  $N \rightarrow \infty$  this equation is transformed exactly into Eq. (10) obtained above for a semi-infinite crystal with surface perturbation at only one surface of the crystal. Indeed, since in the limit  $N \rightarrow \infty$  the fraction in the second and in the last terms in Eq. (10) transforms into  $\exp(-\varphi)$  and  $\exp(-2\varphi)$ , respectively, the Eq. (24) may be rewritten as  $[1 + \kappa \exp(-\varphi)]^2 = 0$ . This is then equivalent to Eq. (10). Therefore, we come to the natural result that the magnetic structure in the surface region of a semi-infinite crystal is not affected by the boundary condition at the other surface of this crystal. Second, Eq. (24) is quadratic with respect to parameter  $\kappa$  and thus may be solved analytically. The expression for the root  $\kappa$  of Eq. (24) corresponding to minimal eigenvalue  $\lambda$  is given by

$$\begin{aligned} -\kappa &= \exp(\varphi) + \left[ -\frac{\sinh \varphi}{\sinh \varphi(N-1)} \{1 + \exp[-\varphi(N-1)]\} \right] \\ &\approx \exp(\varphi) + [-2 \sinh \varphi \exp(-\varphi\{N-1\})]. \end{aligned} \quad (25)$$

The rectangular brackets contain the correction to our previous result, Eq. (10), obtained for semi-infinite crystal in the limit  $N \rightarrow \infty$ . As it follows from Eq. (25) this correction decreases exponentially with the thickness of the film. More importantly, this correction is negative in the interval  $0 < \varphi < \infty$ . This gives rise to the following consequence: Equation (25) is satisfied with a larger magnitude of  $\varphi$  for any given value of the parameter  $-\kappa$ . Therefore, one may conclude that in contrast to the result obtained for thin films supported on a hard magnetic substrate, accounting for a finite number of layers in a thin film supported on a nonmagnetic substrate gives rise to an increase in the parameter  $\varphi$ . As a consequence, the minimal eigenvalue  $\lambda$  is decreased and  $\lambda$  crosses zero earlier compared to a semi-infinite crystal. In other words, in order to satisfy the requirement  $\lambda = 0$ , one needs a smaller surface anisotropy compared to that of semi-infinite crystal. Therefore, SMC is enhanced in a thin film supported on a nonmagnetic substrate relative to a film on a hard magnetic substrate. This situation is illustrated in Fig. 6.

Below we evaluate this solution for a few different film thicknesses  $N$ .

$N = 1, 2$ . In these cases, the bulk layers are absent and thus the problem is ill defined because the concept of canting magnetic structure cannot be applied to these systems. The

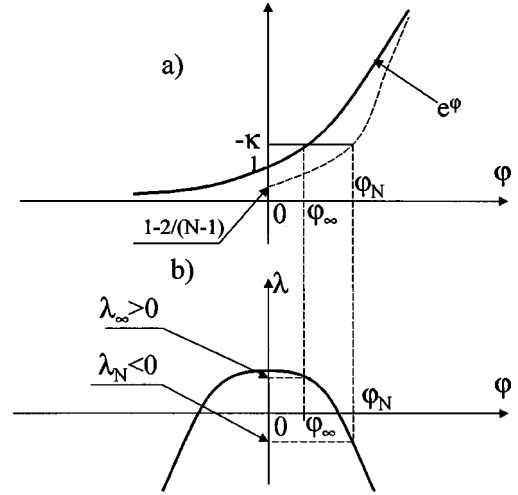


FIG. 6. (a) Graphical solution of Eq. (10) for the parameter  $\varphi$  corresponding to minimal eigenvalue of the matrix  $A$  in Eq. (5) for a semi-infinite ferromagnet (solid line) and Eq. (25) for an  $N$ -layer film supported on a nonmagnetic substrate (dashed line). (b) Graphical illustration of the case when the criterion for SMC in a semi-infinite ferromagnet is not fulfilled ( $0 < \lambda_\infty$ ), but in an  $N$ -layer film with the same magnitudes of model parameter  $k_S, k_B$  fulfilled ( $\lambda_N < 0$ ). The enhancement of SMC region in the phase ( $k_S, k_B$ ) diagram for thin magnetic films supported on a nonmagnetic substrate compared to semi-infinite crystal is essentially a thin-film effect. The additional effective perpendicular anisotropy in such film exists exclusively because of the lack of inner layers exhibiting an in-plane anisotropy due to finite thickness of thin film. This effect cannot be assigned either to the surface-anisotropy constant or to the bulk one and thus needs to be accounted for directly in the treatment of SRT in thin films supported on a nonmagnetic substrate.

orientation of the vector moment of these films is totally determined only by the sign of surface anisotropy constant  $K_S$ , i.e., it is parallel to the film plane when  $K_S > 0$  and it is perpendicular to the film plane when  $K_S < 0$ .

$N = 3$ . If  $k_S < -1$ , SMC takes place whenever  $k_B > 0$ , while for  $k_S > -1$  the SMC occurs only when  $k_B$  satisfies the inequality

$$k_B < \frac{-2k_S}{k_S + 1}. \quad (26)$$

The right side of Eq. (26) is bigger than that of Eq. (13) and thus in this case, the region of SMC is larger than that of a semi-infinite crystal. Similar to the case of the semi-infinite crystal, the SMC/in-plane border goes through the origin  $k_S = 0, k_B = 0$ .

$N = 4$ . Similar to the case  $N = 3$ , for  $k_S < -1$  SMC occurs whenever  $k_B > 0$ . For  $k_S > -1$  SMC takes place only if  $k_B$  satisfies the inequality

$$k_B < -\frac{k_S}{k_S + 1}. \quad (27)$$

The right side of Eq. (27) is smaller than that of Eq. (26) obtained for  $N = 3$ , but larger than that of Eq. (13), which determines the SMC/in-plane border for a semi-infinite crys-

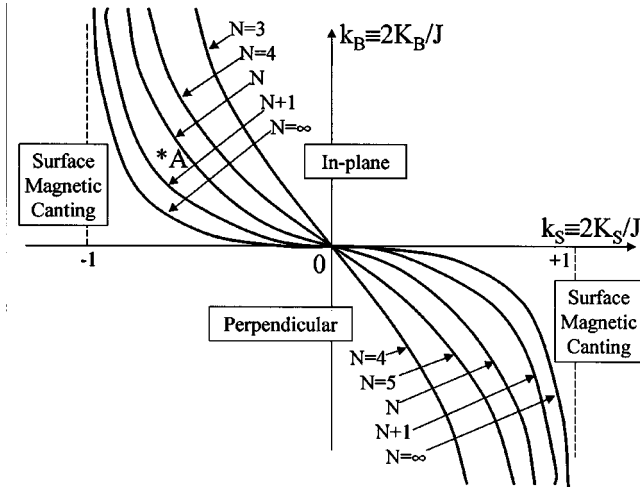


FIG. 7. Evolution of SMC/in-plane and SMC/perpendicular borders in the  $(k_S, k_B)$  phase diagram with the increase in thickness of a thin film supported on a nonmagnetic substrate. Point A in the left upper corner of the phase diagram is located in the SMC region for an  $N$ -layer film. However, the point A with the same coordinates  $(k_S, k_B)$  is located in an in-plane region for an  $(N+1)$ -layer film. This illustrates the SRT from SMC in the  $N$ -layer film to an in-plane uniform magnetic structure of the  $(N+1)$ -layer film with the increase in thickness.

tal. Therefore, in this case the SMC region is smaller than that of the case  $N=3$  but bigger than that of the semi-infinite crystal. The SMC/in-plane border has a  $k_B$  intercept at the origin.

$N=5$ . Similar to the cases  $N=3$  and  $N=4$ , for  $k_S < -1$  SMC occurs whenever  $k_B > 0$ . For  $k_S > -1$  the evolution of the border is the same, i.e., the SMC region shrinks and the SMC/in-plane border goes through the origin. The SMC region is determined by the inequality

$$k_B < \frac{-3 - 2k_S + \sqrt{8k_S^2 + 16k_S + 9}}{2(k_S + 1)}. \quad (28)$$

A common feature of all the lines that determine the SMC/in-plane border in the phase diagram for thin films supported on the nonmagnetic substrate is that each of these lines has an asymptote at  $k_S = -1$  and goes through the origin  $k_S = 0, k_B = 0$  (Fig. 7). This line moves to the left in the  $(k_S, k_B)$  diagram as  $N$  increases. In the limiting case  $N \rightarrow \infty$  the SMC/in-plane border coincides with that obtained for the semi-infinite crystal. This result also may be treated as a qualitative description of a SRT in a thin film as the thickness increases. Indeed, while an  $N$ -layer film exhibits SMC, the  $(N+1)$ -layer film with the same  $k_S$  and  $k_B$  exhibits an in-plane orientation. Therefore, contrary to the result obtained in case (A) we find an inverse SRT from SMC to an in-plane orientation with increasing thickness of a thin film supported on nonmagnetic substrate.

These results may be understood in the following way. Similar to the case of a thin film supported on a hard magnetic substrate, the existence of the asymptote at  $k_S = -1$  in each curve for  $N=3, 4, 5, \dots$  shows that the surface vector

moment is always canted when the surface anisotropy exceeds the exchange interaction with the subsurface layer. In this case SMC always exists. The enhancement of the SMC region for the thin film supported on a nonmagnetic substrate compared to that of a semi-infinite crystal takes place due to the lack of bulk layers that exhibit an in-plane anisotropy. On the contrary, the decrease in the SMC region with the thickness takes place due to the increase in the number of inner layers that exhibit an in-plane anisotropy and thus promote the in-plane orientation.

The generalization of this result for the case of bulk anisotropy  $K_B$  that favors magnetization perpendicular to the surface and the surface anisotropy favoring in-plane magnetization ( $k_S < 0, k_B < 0$ ) is straightforward.

Computer simulations were run to verify these results. We chose a number of atomic layers,  $N$ , whose vector moments were allowed to deviate from the surface plane for  $k_S < 0, k_B < 0$  (from normal to the surface for  $k_S > 0, k_B < 0$ ) and minimized the expression for the energy in Eq. (1). This procedure allowed us to obtain numerical data for  $\sin(\theta_n)$  ( $n=1, 2, 3, \dots, N$ ). The number of atomic layers  $N$  was then varied until  $\sin(\theta_N) < 10^{-3}$ . These simulations confirmed that the analytical results presented above are accurate. In addition, it was confirmed that all borders that separate different regions in the phase diagram correspond to second-order phase transitions. This result verifies that the expansion of the energy in Eq. (1) is appropriate with respect to small variations in  $\theta_n$  according to Eq. (2).

## V. CONTINUUM APPROACH

To date the problem of SMC of a semi-infinite ferromagnet has been considered only within a continuum approach.<sup>2,3</sup> This approach disregards the layered nature of the substance and reduces the problem to the solution of a differential equation with a boundary condition at the surface plane. This approach has a significant advantage because it allows one to get the dependence of the angle  $\theta$  on distance from the surface analytically. Here we revisit this approach and show that it is necessary to include higher-order effects to match the exact, discrete solution. For the sake of simplicity, we restrict ourselves to the consideration of the case of a semi-infinite ferromagnet exhibiting in-plane anisotropy in the bulk ( $k_B > 0$ ) and perpendicular anisotropy in the surface ( $k_S < 0$ ). In brief, the procedure for finding the canting profile  $\theta(z)$  is the following.

Minimization of the energy in Eq. (1) with respect to each angle  $\theta_n$ , for  $n=2, 3, 4, \dots$ , gives rise to an infinite set of similar equations,

$$\frac{\partial E}{\partial \theta_n} = -J \sin(\theta_{n-1} - \theta_n) + J \sin(\theta_n - \theta_{n+1}) + K_B \sin 2\theta_n = 0. \quad (29)$$

The equation obtained after the minimization of energy in Eq. (1) with respect to the angle  $\theta_1$  differs from Eq. (29) and is given by

$$\frac{\partial E}{\partial \theta_1} = J \sin(\theta_1 - \theta_2) + K_S \sin^2 2\theta_1 = 0. \quad (30)$$

The essential feature of the continuum approach is that the difference between the angles of adjacent layers is postulated to be small, and thus the following approximations are assumed to be valid

$$\theta_{n+1} \approx \theta_n + \theta'_n + \frac{1}{2} \theta''_n, \quad \sin(\theta_{n+1} - \theta_n) \approx \theta_{n+1} - \theta_n. \quad (31)$$

This reduces the problem of the description of SMC to the solution of a second-order differential equation

$$\theta''(z) - \frac{1}{2\xi^2} \sin 2\theta(z) = 0 \quad (32)$$

with the boundary condition at the surface plane

$$\theta'(0) - \frac{k_S}{2} \sin 2\theta(0) = 0. \quad (33)$$

Here we have shifted the enumeration of the atomic layers, and  $n=1$  corresponds to  $z=0$ . The parameter  $\xi$  introduced in Eq. (32) is determined by the formula  $1/k_B = \xi^2$ .

The solution of Eq. (32) has the form

$$\tan \frac{\theta(z)}{2} = \tan \frac{\theta(0)}{2} \exp\left(-\frac{z}{\xi}\right), \quad (34)$$

and thus  $\xi$  is the effective depth of the canting profile. The boundary condition Eq. (33) gives

$$\cos \theta(0) = -\frac{J}{2\xi K_S} \equiv -\frac{\sqrt{k_B}}{k_S}. \quad (35)$$

It follows from this formula that the SMC of a ferromagnet exhibiting in-plane anisotropy in the bulk takes place if the requirement  $|\cos \theta(0)| < 1$  is satisfied. The solution of this inequality gives  $k_B < k_S^2$ . Similar consideration of the case  $k_S > 0$ ,  $k_B < 0$  gives rise to the inequality  $-k_S^2 < k_B$ . Both plots  $k_B = k_S^2$  and  $k_B = -k_S^2$  are presented in Fig. 8 by dashed lines. It follows that this approximation of the continuum approach does not imply the existence of regions where SMC exists regardless of how large the in-plane bulk-anisotropy constant is, which is a nonphysical result, as described above. Indeed, in the phase diagram presented in Fig. 8, the SMC region obtained within the continuum approach is restricted from above by the parabola  $k_S = k_B^2$  for any magnitude of  $k_S$ .

To simplify the comparison of these results with ours, we expand the right side of the inequality in Eq. (13) exhibiting our criterion for SMC in the vicinity of  $k_S = 0$ . This expansion gives rise to the formula

$$k_B < k_S^2 - k_S^3 + k_S^4 - k_S^5 + \dots \quad (36)$$

This result shows that the continuum approach ( $k_B < k_S^2$ ) accounts for only the first term in Eq. (36) and thus is not accurate. As a consequence, it leads to an overestimation of surface anisotropy. Indeed, as it follows from Eq. (36) and

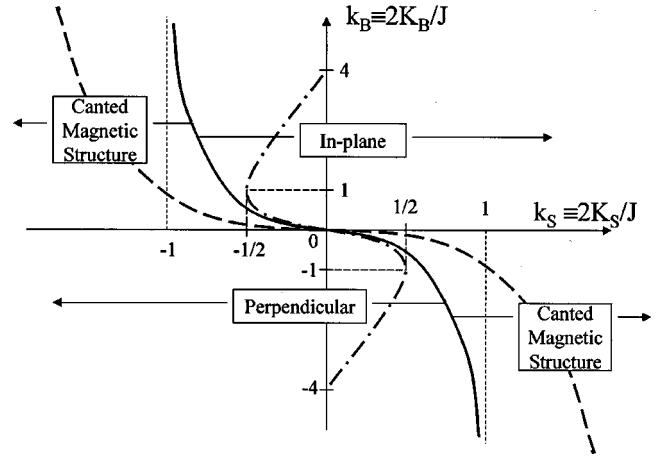


FIG. 8. Magnetic phase diagram obtained here (solid line), Eqs. (13) and (15). Magnetic phase diagram corresponding to the continuum approach of Ref. 2 (dashed line), Eq. (35). The improved continuum-approach magnetic phase diagram obtained by including the second derivatives in the boundary condition according to Eq. (33) (dashed-dotted line), Eq. (41).

also from Fig. 6 within the approach used in the present article for given bulk anisotropy  $k_B > 0$ , the SMC appears for smaller surface anisotropy compared to what the continuum approach gives. The relative error is given by

$$\frac{1}{2}(\sqrt{k_B + 4} + \sqrt{k_B}) - 1. \quad (37)$$

The magnitude of  $k_B$  is small for metals such as Fe, Co, Ni. It may be estimated from the domain-wall thickness  $\xi$  because  $k_B = 1/\xi^2$ . According to Ref. 8,  $\xi$  (in terms of lattice parameters) is 138, 36, and 285 for Fe, Co, and Ni, respectively. For Fe, this formula gives a difference of 1.4%. Therefore, the error determined by Eq. (36) is small for these natural magnets. On the other hand, artificially created multilayers demonstrate substantial variations in vector-moment orientation across the films on the atomic scale, and thus one may expect more substantial variations in the coordinates of the point  $(k_S, k_B)$  in the phase diagram. We shall demonstrate this in the next section.

The discrepancies between our results and those obtained with the continuum approach originate from an inconsistency in the form of the continuum approach used in Refs. 2 and 3. The problem is that while the differential equation of Eq. (30) was obtained including the second derivative in Eq. (31), the boundary condition of Eq. (33) implies that the second derivative is ignored. We believe that this is not appropriate in the vicinity of the surface, where the difference between angles is larger than in the bulk. As a consequence, one must take the second-derivative term into account while treating the boundary condition at the surface plane.

Accounting for the second derivative, Eq. (31), in the expansion of Eq. (30) gives rise to another boundary condition at the surface plane,

$$\frac{1}{2} \theta''(0) + \theta'(0) - \frac{k_S}{2} \sin 2\theta(0) = 0. \quad (38)$$

The intermediate solution of the differential equation (32) may be written in the form

$$\theta'(z) = -\frac{\sin \theta(z)}{\xi}. \quad (39)$$

Also, as it follows from Eq. (32),

$$\theta''(z) = \frac{1}{2\xi^2} \sin 2\theta(z). \quad (40)$$

Equations (39) and (40) being substituted in Eq. (38) give rise to the result

$$\cos \theta(0) = \frac{2\sqrt{k_B}}{k_B - 2k_S}. \quad (41)$$

The analysis of this formula shows that accounting for the second derivative in the boundary condition Eq. (38) leads to the existence of a region in the  $(k_S, k_B)$  phase diagram where the surface is canted regardless of the magnitude of  $k_B$ . The SMC/in-plane border is presented in Fig. 8 by a dashed-dotted line. As one can see from this picture, the result obtained is still not perfect because, according to Eq. (41), the region where the surface is always canted takes place for  $k_S < -\frac{1}{2}$  rather than  $k_S < -1$ . Also, the increase in  $k_B$  for  $-\frac{1}{2} < k_S < 0$  leads to a SRT from SMC to an in-plane structure and then to another SRT from the in-plane structure to SMC. This again gives a nonphysical result. On the other hand, Eq. (41) is more accurate than Eq. (35) for small magnitudes of  $k_B$  and  $k_S$ .

To summarize the results of this comparison, we conclude that the discrete method used here for constructing the phase diagrams for SMC in semi-infinite magnets is more consistent than the continuum approach. In contrast to the continuum approach, this method allows one to consider thin-film magnetism and to describe the SRT from in-plane to SMC in ultrathin films supported on hard magnetic substrates and the inverse SRT in ultrathin films supported on non magnetic substrates (see Sec. IV). We have to mention that our computer simulations with artificially restricted numbers of atomic layers ( $N=1, 2, 3, 4$ ) that are allowed to deviate their vector moment from an in-plane orientation demonstrate that the canting profile through the thickness of these ultrathin films is substantially nonuniform. Since the continuum approach cannot be applied to the treatment of thin-film magnetism, it is better to obtain canting profiles by direct minimization of the energy with the help of a computer rather than using the continuum approach as was done in Ref. 2.

## VI. THE TREATMENT OF SRT OBSERVED IN 1.5 ATOMIC LAYERS Fe/Gd WITHIN THE DISCRETE APPROACH

Recently we reported on the two-step SRT in 1.5 atomic layers (AL) of Fe on Gd with temperature discovered with spin polarized secondary electron-emission spectroscopy.<sup>9</sup> It was shown that the first step in the SRT observed is a second-order phase transition from an in-plane orientation of

the Fe vector moment to the canting state. The next step is an irreversible first-order phase transition to another canting state with a larger deviation of the Fe vector moment from the in-plane orientation. Later experimental investigations of this system were performed using the magneto-optic Kerr effect (MOKE).<sup>10</sup> Because of its greater penetration depth, the MOKE shows both the Fe and Gd film response, as opposed to the spin polarized electrons, which are sensitive only to the top surface layer. Results obtained by means of MOKE show unequivocally that the Gd atomic layers in the surface region take part in the SRT, and thus this system is a realization of SMC structure.

As it follows from these experiments, the ground state at low temperature is an in-plane magnetic structure. The increase in temperature gives rise to a SRT from an in-plane to SMC structure. Therefore, we must choose  $K_S < 0$  and  $K_B > 0$  and treat the SRT observed within the left upper part of the phase diagram in Fig. 2. This is done within the following assumptions.

(1) Since the SRT takes place within a narrow temperature interval close to the Gd Curie temperature, 270–290 K, one must assume that the Gd magnetization  $M_{\text{Gd}}$  and also its easy-plane anisotropy energy strongly depend on temperature and decrease to zero in the vicinity of the Gd Curie point.

(2) Since the Curie point of the Fe film (400 K) is far above the Gd Curie point (292 K), the Fe magnetization  $M_{\text{Fe}}$  and its easy-axis anisotropy energy is assumed to be temperature independent in the narrow temperature interval 270–290 K. The energy of the Fe-Gd exchange interaction is taken to go to zero in the vicinity of the Gd Curie point because it is proportional to the product  $M_{\text{Fe}}M_{\text{Gd}}$ . Here we do not take polarization effects into account.

(3) Since 1.5-AL Fe/Gd is a nonuniform system, we must generalize the results obtained in the previous sections. First, the Fe-Gd exchange interaction  $J_{\text{Fe-Gd}}$  is assumed to be larger than Gd-Gd exchange interaction  $J_{\text{Gd-Gd}}$ . And second, in the vicinity of the Gd Curie point, the Fe layer magnetization  $M_{\text{Fe}}$  is assumed to be both much bigger than the Gd layer magnetization  $M_{\text{Gd}}$  and also independent of temperature. As a consequence, the scalar surface perturbation  $\kappa$  in Eq. (5) transforms into a matrix. The procedure for evaluating the criterion for the nonstability of the uniform in-plane structure is similar to that presented in Sec. I.

Within these three assumptions, the criterion for SMC is given by

$$k_B < -\frac{k_S + 1}{(\gamma - 1)k_S - 1} - 2 - \frac{(\gamma - 1)k_S - 1}{k_S + 1}, \quad (42)$$

where

$$\gamma = \frac{J_{\text{Fe-Gd}}M_{\text{Fe}}}{J_{\text{Gd-Gd}}M_{\text{Gd}}}, \quad k_S = \frac{2K_S M_{\text{Fe}}}{J_{\text{Fe-Gd}}M_{\text{Gd}}}, \quad k_B = \frac{2K_B}{J_{\text{Gd-Gd}}}. \quad (43)$$

First, it follows from Eq. (42) that if  $\gamma$  is set to 1, then it coincides with Eq. (13), which was obtained with the assumption that the film is uniform. Second, since the increase in temperature leads to the decrease of  $M_{\text{Gd}}$  to zero, according to Eq. (43), the magnitudes of the parameters  $\gamma > 0$  and

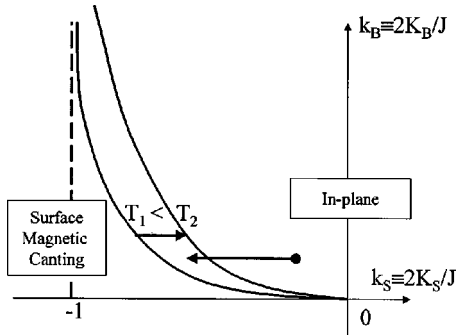


FIG. 9. The part of magnetic phase diagram generalized for the case of nonuniform films according to Eq. (34). The increase in temperature leads to the movement of the SMC/in-plane border to the right side of the diagram shown by an arrow oriented to the right. The SMC/in-plane border is presented for two temperatures  $T_1$  and  $T_2 > T_1$ . The point corresponding to 1.5-AL Fe/Gd moves with temperature to the left (shown by a single arrow oriented to the left). The meeting of this point and the SMC/in-plane border signifies second-order SRT observed experimentally in Refs. 9 and 10.

$k_S < 0$  will approach positive and negative infinity, respectively. The analysis of Eq. (42) shows that for  $\gamma > 2$  and  $k_S < 0$  the right side of Eq. (42) increases with temperature due to the increase of the parameter  $\gamma$ . As a consequence, the SMC/in-plane border moves to the right in the  $(k_S, k_B)$  phase diagram. Also, the point in the in-plane region of the  $(k_S, k_B)$  phase diagram corresponding to 1.5-AL Fe/Gd at low temperature moves to the left with temperature due to the increase in the absolute value of  $k_S < 0$ . Therefore, this point

and the SMC/in-plane border move towards each other with temperature. The point corresponding to the 1.5-AL Fe/Gd will necessarily cross the in-plane/SMC border with temperature and the system will undergo a SRT to the canted state via a second-order phase transition, as observed experimentally. The phase diagram generalized for the case of the nonuniform system according to Eq. (42) is presented in Fig. 9.

Thus we demonstrate, as it was mentioned in Sec. V, that multilayer systems exhibit a more substantial variation in the reduced anisotropy coordinates  $k_S, k_B$  than uniform magnets such as Fe, Co, and Ni. In particular, the reduced surface anisotropy  $k_S$  can exist in the region where  $k_S < -1$ , and SMC exists regardless of how large the bulk reduced anisotropy  $k_B$  is.

The description of the first step of the SRT in 1.5-AL Fe/Gd presented above may be considered only as a first step in the full description of this complicated two-step SRT. The problem is that this treatment ignores the fact that the SRT observed experimentally is effectively a two-step transition consisting of a second-order phase transition and a subsequent first-order transition. In order to describe a first-order SRT, one must consider higher-order anisotropy constants. All this is beyond of the scope of the present article.

#### ACKNOWLEDGMENTS

We thank NATO for support of this work under collaborative linkage Grant No. WPST.CLG.976845. A.P.P. also thanks NIST for continued support. We thank C. S. Arnold, P. Dowben, and M. Farle for useful discussions.

<sup>1</sup>L. Néel, J. Phys. Radium **15**, 225 (1954).

<sup>2</sup>D. L. Mills, Phys. Rev. B **39**, 12 306 (1989).

<sup>3</sup>R. C. O'Handley and J. P. Woods, Phys. Rev. B **42**, 6568 (1990).

<sup>4</sup>J. Mathon, Rep. Prog. Phys. **51**, 1 (1988).

<sup>5</sup>T. Kaneyoshi, J. Phys.: Condens. Matter **3**, 4497 (1991).

<sup>6</sup>M. Farle, Rep. Prog. Phys. **61**, 755 (1998).

<sup>7</sup>A. P. Popov and D. P. Pappas, Phys. Rev. B **56**, 3222 (1997).

<sup>8</sup>D. Jiles, *Introduction to Magnetism and Magnetic Materials* (Chapman and Hall, London, 1991), p. 134.

<sup>9</sup>C. S. Arnold, D. P. Pappas, and A. P. Popov, Phys. Rev. Lett. **83**, 3305 (1999).

<sup>10</sup>C. S. Arnold, D. P. Pappas, and A. P. Popov, J. Appl. Phys. **87**, 5478 (2000).